NMRlipids IV: Headgroup & glycerol backbone structures, and cation binding in bilayers with PE and PG lipids

Pavel Buslaev,[1] Fernando Favela-Rosales,[2] Patrick Fuchs,[3] Matti Javanainen,[4] Jesper J. Madsen,[5,6] Josef Melcr,[4,7] Markus S. Miettinen,[8] O. H. Samuli Ollila,[9,*] Chris G. Papadopoulos,[10] Antonio Peón,[11] Thomas J. Piggot,[12] and Pierre Poulain[3]

[1]*University of Jyväskylä*
[2]*Departamento de Investigación, Tecnológico Nacional de México, Campus Zacatecas Occidente, México*
[3]*Paris, France*
[4]*Institute of Organic Chemistry and Biochemistry of the Czech Academy of Sciences, Flemingovo nám. 542/2, CZ-16610 Prague 6, Czech Republic*
[5]*Department of Chemistry, The University of Chicago, Chicago, Illinois, United States of America*
[6]*Department of Global Health, College of Public Health, University of South Florida, Tampa, Florida, United States of America*
[7]*Groningen Biomolecular Sciences and Biotechnology Institute and The Zernike Institute for Advanced Materials, University of Groningen, 9747 AG Groningen, The Netherlands*
[8]*Department of Theory and Bio-Systems, Max Planck Institute of Colloids and Interfaces, 14424 Potsdam, Germany*
[9]*Institute of Biotechnology, University of Helsinki*
[10]*I2BC - University Paris Sud*
[11]*Spain*
[12]*Chemistry, University of Southampton, Highfield, Southampton SO17 1BJ, United Kingdom*

(Dated: November 12, 2020)

Abstract

INTRODUCTION

PE and PG lipids are most common lipids in bacteria [1]. Zwitterionic PE is the second most abundant glycerophospholipid in eukaryotic cells and has been related to the diseases [2–4]. Anionic PG lipids are less abundant, but is also proposed to be fundamental for terrestrial life [5]. PE and PG affect membrane protein functionality [6] and bind to various proteins [7]. PE headgroup is also prone for negative membrane curvature and causes membrane fusion [3, 8]. Therefore, the PE and PG headgroup structures play probably essential roles in many biological processes.

Structural details of lipid headgroups are mainly studied using NMR experiments, which suggest that the glycerol backbone structures are largely similar irrespectively of the headroup [9], glycerol backbone and headgroup structure and behaviour are similar in model membranes and in bacteria [9–11], and the headgroup structures are similar in PC, PE and PG lipids, while headgroup is more rigid in PS lipids [12, 13]. Some attempts to resolve conformational ensembles from NMR for PC and PE lipids have been made, but lesser extend for PG or PS lipids [14–16]. Classical molecular dynamics simulations could potentially give such ensembles and therefore enable the detailed studies of lipid headgroup behaviour in complex biomolecular systems, but current force fields are not accurate enough to reproduce the correct conformational ensembles for PC and PS headgroups [17, 18]. Several MD simulations of PE and PG lipids have been published especially in the context of modeling inner membrane of Gram-negative bacteria [19–31] **1.There may be some relevant publication missing from here**, but evaluation of glycerol backbone and headgroup structures against experiments is rare [25].

Besides the structure, also ion binding may regulate biophysical activity of especially negatively charged lipid headgroups [11]. Monovalent cation (except Lithium) binding to zwitterionic PC and anionic PS headgroups is very weak, while multivalent ion binding is stronger but still weak [18, 32–35]. The ion binding affinity data for PE is more scarce [36], but large differences to PC would be surprising. Negatively charged lipids are suggested to bear same cation binding constants than zwitterionic lipids, but the amount of bound ions to negatively charged membranes would still be larger because the concentration of cations in the vicinity of membranes would be higher [11]. On the other hand, anionic PS lipids are proposed chelate with calcium ions [37–39]. In simulations, the cation binding affinity to PC and PS membranes is typically overestimated [18, 35], which can be improved by applying the ECC to the partial charges of the force fields [40, 41].

Here, we use open collaboration and order parameters of glycerol backbone and headgroup to evaluate the accuracy of PE and PG heagroup structures, and the cation binding affinity to anionic membranes containing PG lipids in the current MD simulation force fields. The force field giving the best description for glycerol backbone and headgroup structures of PC, PS, PG and PE headgroups (CHARMM36) reproduces the essential differences in order parameters between these headgroups, and therefore enables the analysis of structural differences between the headgroups.

METHODS

Experimental C–H bond order parameters

The headgroup and glycerol backbone C–H bond order parameter magnitudes and signs of POPE and POPG were determined by measuring the chemical-shift resolved dipolar splittings with a R-type Proton Detected Local Field (R-PDLF) experiment [42] and S-DROSS experiments [43] using natural abundance ^{13}C solid state NMR spectroscopy as described previously [44, 45]. POPE and POPG powder were purchased from Avanti polar lipids. The NMR experiments were identical to our previous work [18]. **2.Is this enough and correct, or should we repeat some methods from the NMRlipidsIVps paper?** The POPE experiments were recorded at 310 K and POPG experiments at 298 K, where the bilayers are in the liquid disordered phase [46].

Absolute values of the headgroup and glycerol backbone order parameters from PE and PG lipids are measured previously using ^{2}H NMR [9, 12, 47, 48]. Because also the order parameter signs bear essential information about the lipid structures [17, 49], we measured the magnitudes and signs of POPE and POPG C–H bond headgroup and glycerol backbone order parameter in liquid phase using the 2D-RPDLF and S-DROSS experiments, as described previously [18, 44, 45]. For POPE, the glycerol backbone and α-carbon peaks in INEPT spectra were assigned based on previously measured POPC spectra [44] and the β-carbon peak was assigned based on ^{13}C chemical shift table for amines available at `https://www.chem.wisc.edu/areas/reich/nmr/c13-data/cdata.htm` (Fig. S7). For POPG, the glycerol backbone peaks in INEPT spectra were assigned based on previously measured POPC spectra [44], while α and γ-carbon peaks **3.How were these assigned?** (Fig. S8). The numerical value of the β-carbon order parameter could not be determined, because its peak overlapped with the g_2 peak from glycerol backbone in POPG. However, the order parameter of β-carbon is expected to be clearly smaller than for g_2 based on previous ^{2}H NMR measurements [9, 12, 48]. Therefore, the beginning of the S-DROSS curve gives the sign for g_2 order parameter and end for β (Fig. S8 (E)). This is confirmed with SIMPSON calculations using negative value for g_2 and positive value for β order parameter (Fig. S9). **4.Details to be checked by Tiago.**

Molecular dynamics simulations

Molecular dynamics simulation data were collected using the Open Collaboration method [17], with the NMRlipids Project blog (`nmrlipids.blogspot.fi`) and GitHub repository (`github.com/NMRlipids/NMRlipidsIVotherHGs`) as the communication platforms. The simulated systems of pure PE and PG bilayers without additional ions are listed in Tables S1 and S2, and lipid mixtures with additional ions in Table S4. Further simulation details are given in the SI, and the simulation data are indexed in a searchable database available at `www.nmrlipids.fi`, and in the NMRlipids/MATCH repository (`github.com/NMRlipids/MATCH`).

The C–H bond order parameters were calculated directly from the carbon and hydrogen positions using the definition

$$S_{\mathrm{CH}} = \frac{1}{2}\langle 3\cos^2\theta - 1\rangle, \qquad (1)$$

where θ is the angle between the C–H bond and the membrane normal (taken to align with z, with bilayer periodicity in the xy-plane). Angular brackets denote average over all sampled configurations. The order parameters were first calculated averaging over time separately for each lipid in the system. The average and the standard error of the mean were then calculated over different lipids. Python programs that use the MDAnalysis library [50, 51] used for all atom simulations is available in Ref. 52 (`scripts/calcOrderParameters.py`). For united atom simulations, the trajectories with hydrogens having ideal geometry were constructed first using either buildH program [53] or (`scratch/opAAUA_prod.py`) in Ref. 52, and the order parameters were then calculated from these trajectories. This approach has been tested against trajectories with explicit hydrogens and the deviations in order parameters are small [53, 54].

5.BuildH program is now cited with a direct link to the GitHub repo. I think that a release to Zenodo would be nice in the final publication.

6.Maybe we should also shortly discuss here about the reasons for slight dependence of order parameter values on the method used to reconstruct hydrogens?

The ion number density profiles were calculated using the `gmx density` tool of the Gromacs sofware package [55].

Analysis of molecular dynamics simulation data

The big data set of MD simulations was analysed in the NMRlipids databank manner. Unique naming convention for lipid atoms in each force field was defined using the mapping files and analysis for all simulations indexed in NMRlipids databank manner were performed using python codes.

Analysis of lipid conformations bound to proteins

Dihedral angles of all available conformations in the PDB databank were calculated using the API access to the databank.

RESULTS AND DISCUSSION

Conformational ensembles of different lipid headgroups in bulk bilayer

Derivation of different lipid headgroup conformational ensembles in liquid state has been inconclusive due to lack of suitable experimental data and tools to interpret the conformational ensembles. Our experimental order parameters, including the signs, from different lipid headgroups combined with the literature data are shown in Fig. 1. The glycerol backbone order parameters are similar for all the lipids, although they move slightly toward positive values (closer to zero) in the order PC $<$ PE $<$ PS $<$ PG. While the headgroup order parameters are similar for PC and PE lipids, PG and PS lipids exhibit distinct values in comparison with other lipids. In PS headgroup, the α-carbon order parameter exhibits significant forking and the β-carbon has more negative value than in other lipids. In PG headgroup, the α-carbon order parameter is similar to PE and PG, while the positive value of β-carbon is distinct from all the other lipids. Notably, this difference was not observed in previous ^{2}H NMR experiments, because absolute value of β-carbon order parameter is similar in PG, PE and PC lipids and the order parameter signs were not measured [9, 12, 48].

As in previous NMRlipids project results for PC and PS lipids [17, 18], none of the MD simulation force fields correctly captures all the headgroup and glycerol backbone order parameters of PE and PG lipids (Figs. S1 and S2) that would enable a straightforward interpretation of conformational ensembles. Nevertheless, CHARMM36 force field, which gives the results closest to the experiments for all lipids, captures the essential differences between PC, PS, PG and PE headroup order parameters (Fig. 7) with the exception of β-carbon order parameter of PC which is too negative when compared with other lipids or experiments [17].

The conformational ensembles characterized by the distributions of heavy atom dihedral angles show major differences between lipids only for O_α-C_α and C_α-C_β bonds near the end of the headgroup (Fig. 7). These probably explain the slight differences in the angle between headgroup dipole and membrane normal, which decreases in the order PG $>$ PE $>$ PC $>$ PS, although difference between PC and PE may an artefact as the β-carbon order parameter in PC is poorly reproduced by the CHARMM36 force field. Dihedrals of both O-P bonds can freely rotate in all lipids as all possible angles are observed in the distributions. For PS, however, some angles are quite unlikely, possible explaining the more rigid headgroup structures proposed for PS lipids [13, 56]. The eclipsed (0 or 360 degrees) are not present in any other dihedrals, and anti-eclipsed (120 or 240 degrees) are not present in C_α-C_β and g_1-g_2 bonds.

In conclusion, the results suggest that free rotations around O-P bonds decouple the headgroup and glycerol backbone structure and dynamics in similarly in all lipids, althought this rotation is slower in PS lipids where crossing certain barriers are slower. Despite significant differences in dihedral distributions near the headgroup end, all lipids have dihedral angles within approximately the same ranges. This suggests that all lipids can quite freely arrange to multiple headgroup conformations when interaction with proteins, ions or other biomolecules.

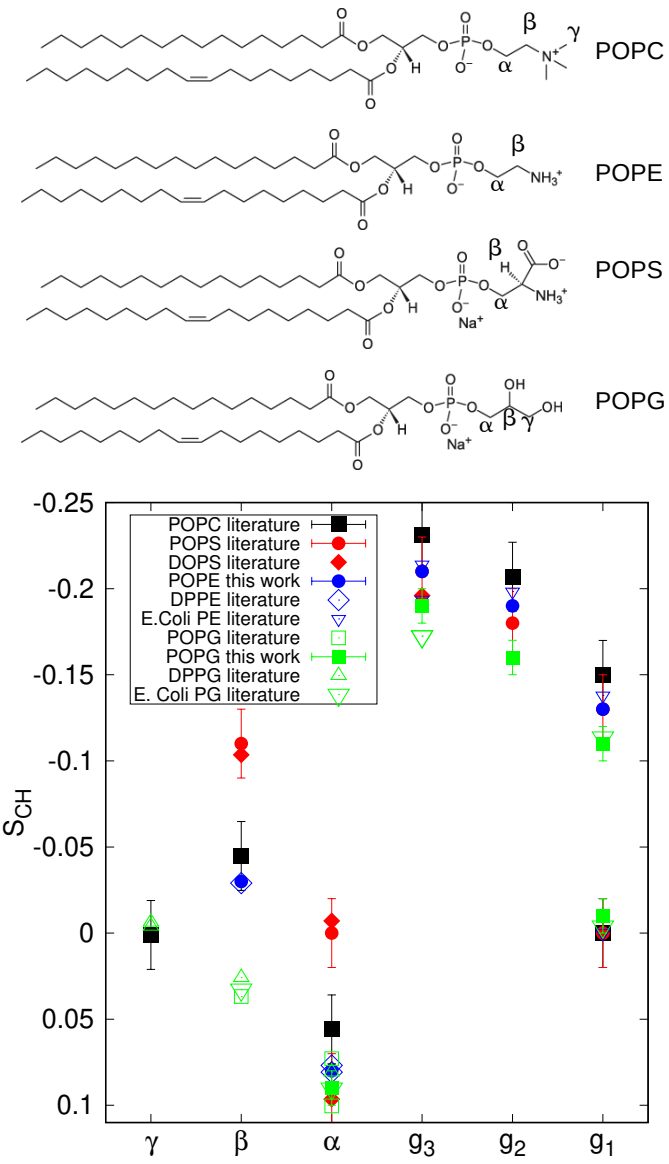

FIG. 1: (top) Chemical structure of different lipids. (bottom) Headgroup and glycerol backbone order parameters from different experiments in lamellar liquid disordered phase. The values and signs for POPE (310 K) and POPG (298 K) measured in this work, and for POPS (298 K) [18] and POPC (300 K) [44, 45] previously using ^{13}C NMR. The literature values for DOPS with 0.1M of NaCl (303 K) [56], POPG with 10nM PIPES (298 K) [48], DPPG with 10mM PIPES and 100mM NaCl (314 K) [12], DPPE (341 K) [47], E.coliPE and E.coliPG (310 K) [9] are measured using ^{2}H NMR. The signs from ^{13}C NMR are used also for the literature values.

7.The bottom figure could be clarified as Fig. 2 in the NMRlipids IVps paper.

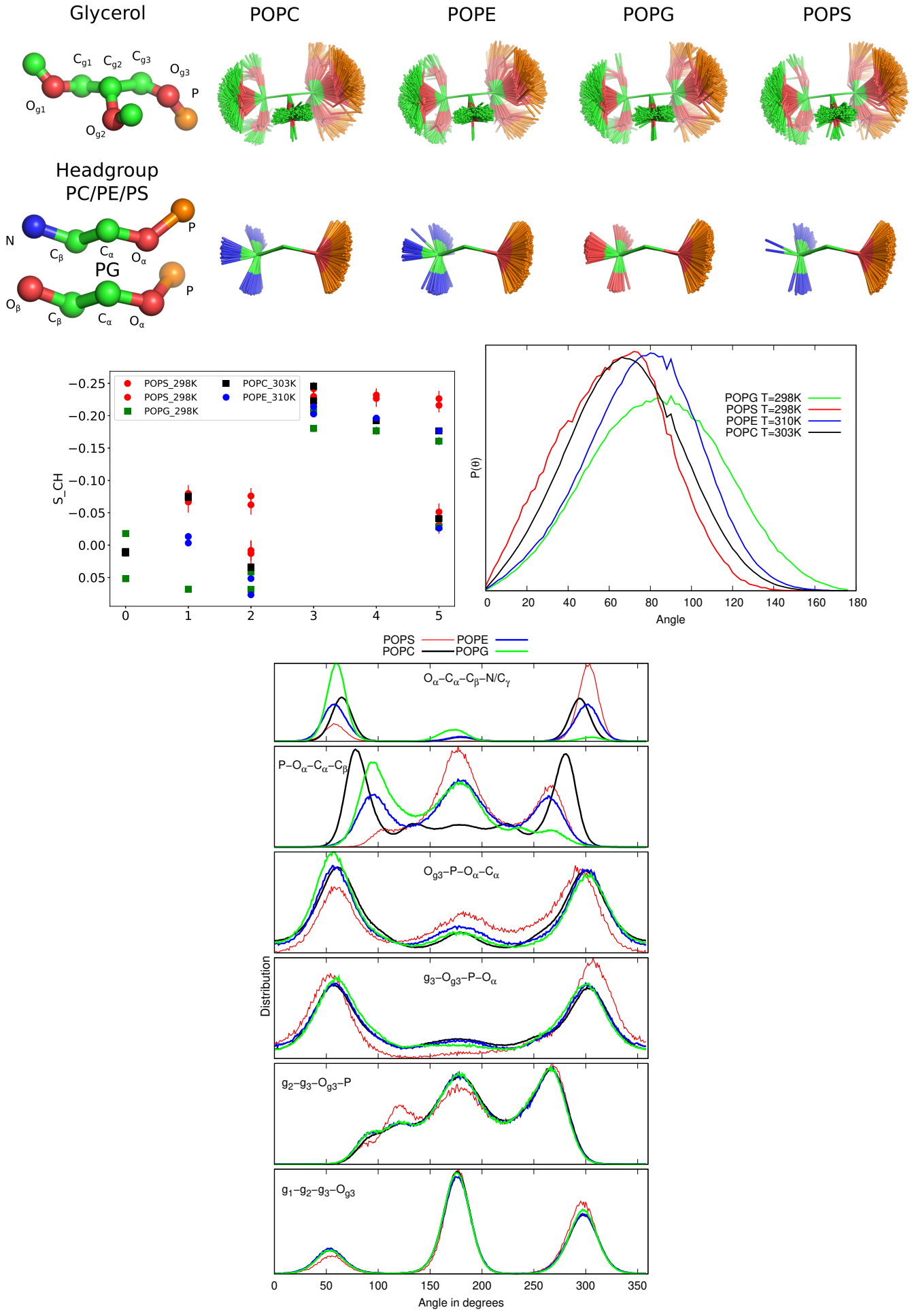

FIG. 2: Overlayed snapshots and dihedral angle distributions from CHARMM36 simulations of different lipids which give the best agreement with experiments.

8.The differences observed in dihedral distributions are not visible in the snapshot figures.

9.More detailed discussion of this figure is in https://github.com/NMRLipids/NMRlipidsIVPEandPG/issues/9

Lipid conformational ensembles in lipid bilayers with bound ions

Headgroup order parameters of PC lipids decrease or increase upon addition of positive or negative charge into membrane, respectively, while they remain unchanged upon addition of neutral molecules such as cholesterol or sphingomyelin [**?**]. This has been explained by the tilting of the headgroup dipole due to electrostatic interactions with bound charges, and has been used to measure the binding affinity of ions to membranes [**?**].

The changes of PC headgroup order parameters in POPC:POPG (1:1) and (4:1) mixtures upon addition of $CaCl_2$ from simulations and experiments [48, 59] in Figs. 3 and S12 are in line with conclusion from our previous studies [**?**]: order parameters decrease in the response to bound cations in qualitative agreement with experiments, but calcium binding affinity to membranes is overestimated in simulations except in CHARMM36 with the NBfix correction which underestimates the binding affinity. On the other hand, implicit inclusion of electronic polarizability to Amber based lipid models improves the ion binding affinity leading to a good agreement with experiments.

Changes in lipid conformational ensembles characterized by distributions of heavy atom dihedral angles are very small upon binding of calcium or addition of cationic surfactants to membranes (Figs. **??**). Yet, such changes are sufficient to tilt the headgroup dipole angle and reproduce the experimentally observed order parameter changes in α and β carbons.

Simulations also qualitatively reproduce the experimentally observed decrease of POPG β-carbon order parameter upon addition of $CaCl_2$, suggesting that the PG headgroup response is qualitatively captured by simulations, in contrast to PS in our previous work [18]. and more modest decrease with larger concentrations (Fig. 3) [48]. This behaviour is similar to that of β-carbon order parameters of POPC, but essentially different than observed for POPS, where β-carbon order parameters increases with addition of calcium [18]. Experimentally measured changes of PG α-carbon order parameters upon addition of calcium are not available. Lipid17 and Slipids force fields correctly capture the PG β-carbon order parameter response to $CaCl_2$ even thought the binding affinity was too large based on the comparison of PC headgroup order parameter changes with experiments. While applying ECC to Lipid17 improved the PC headgroup order parameter response and binding affinity, the response of PG β-carbon order parameter to calcium is too weak in this model. The response of PG α-carbon order parameters to $CaCl_2$ differs between force fields, but experimental data to evaluate these predictions is not available.

10.To be finished once we have the new CHARMM simulations and conformational changes of PG analyzed.

11.We still need more data to finish the discussion. More detailed discussion is in https://github.com/NMRLipids/NMRlipidsIVPEandPG/issues/12

Protein bound lipid conformations

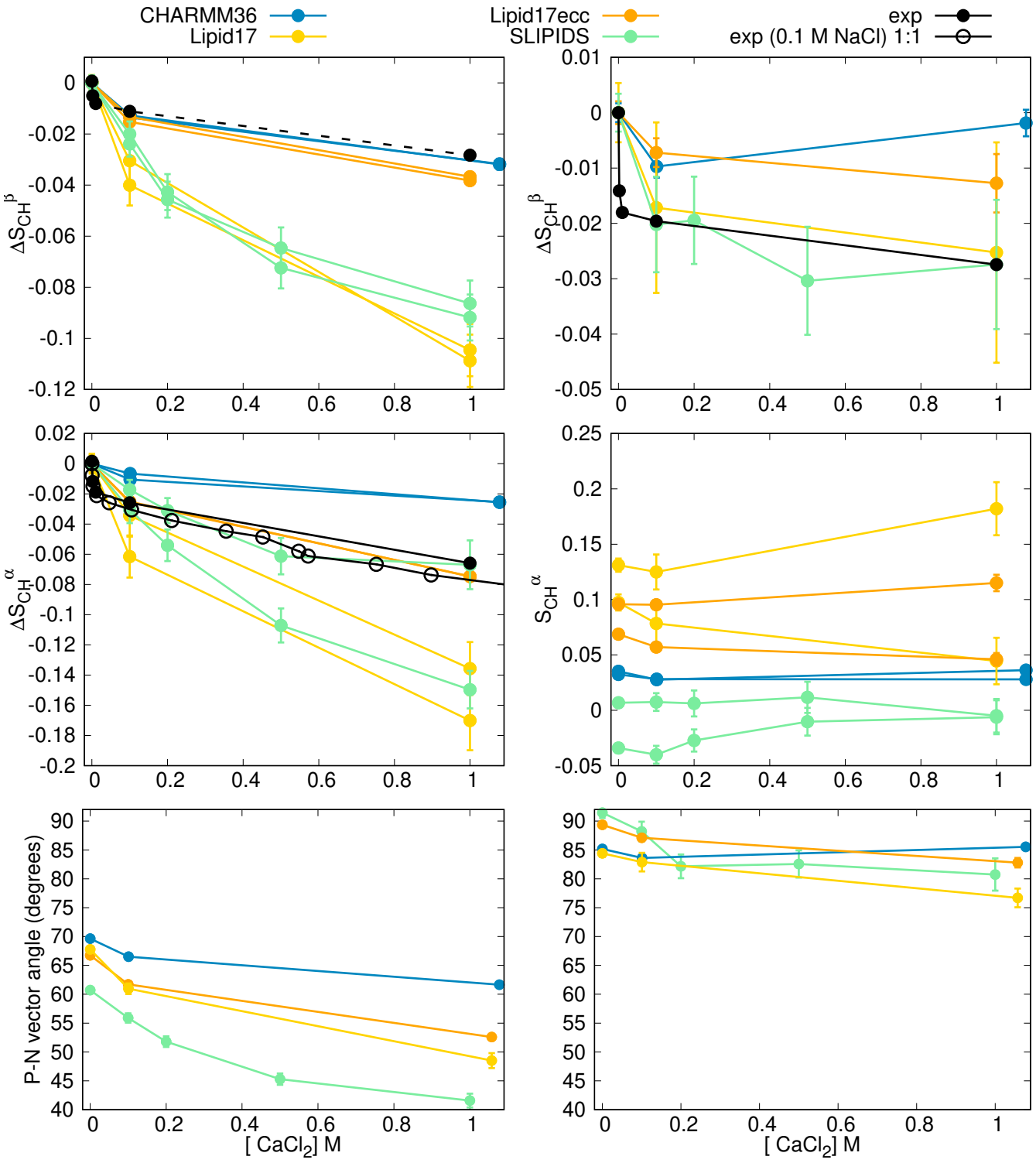

FIG. 3: Modulation of headgroup order parameters of POPC (*left*) and POPG (*right*) in POPC:POPG (1:1) mixture upon addition of $CaCl_2$ in 298 K temperature from experiments [48, 59] and simulations. The β-carbon order parameter of POPC (dashed line on top left) is not directly measured but calculated from empirical relation $\Delta S_\beta = 0.43\Delta S_\alpha$ [60]. The changes with respect to the systems without $CaCl_2$ are shown for other data than for the α-carbon of POPG for which experimental order parameter is not available.

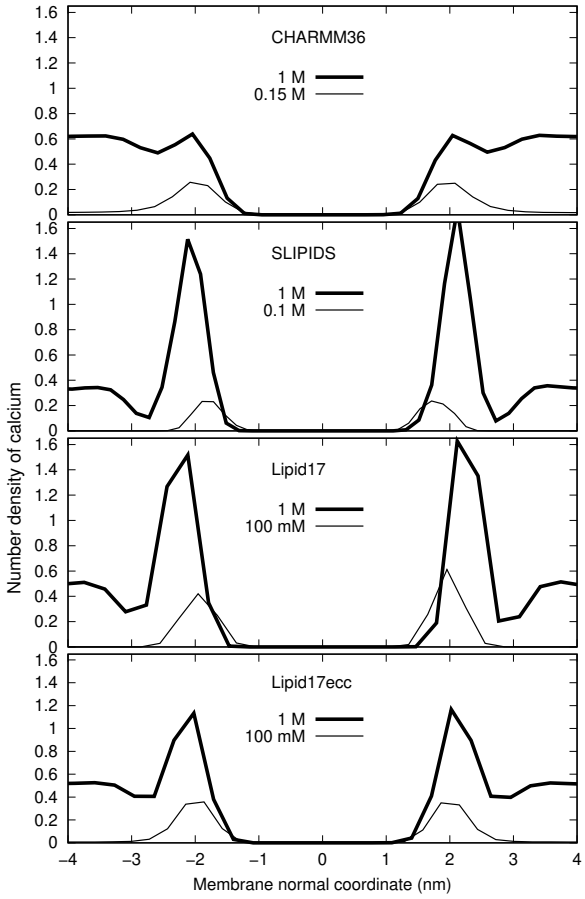

FIG. 4: Calcium ion density profiles along membrane normal from simulations of POPC:POPG (1:1) mixtures with different force fields.

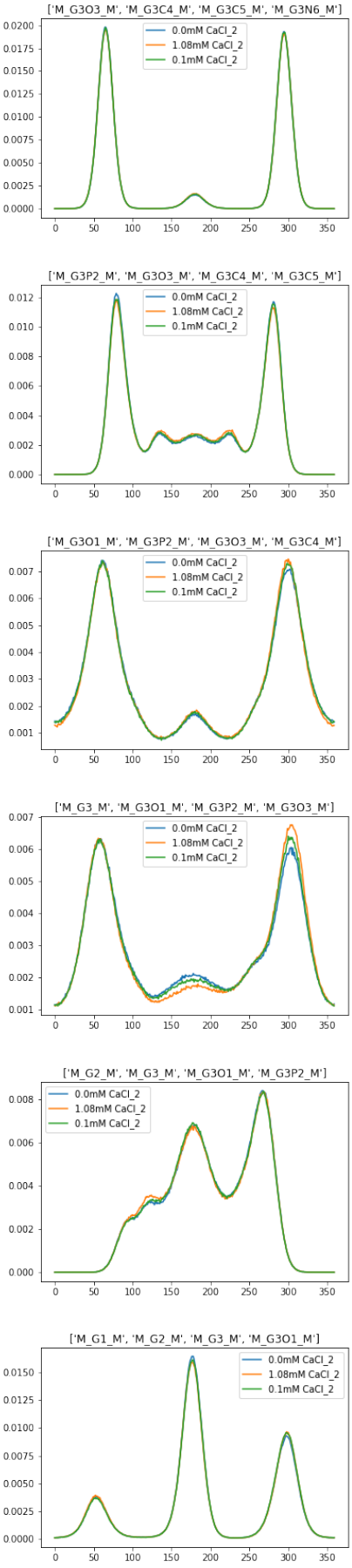

FIG. 5: Changes in POPC CHARMM36 dihedrals with increasing amount of $CaCl_2$.

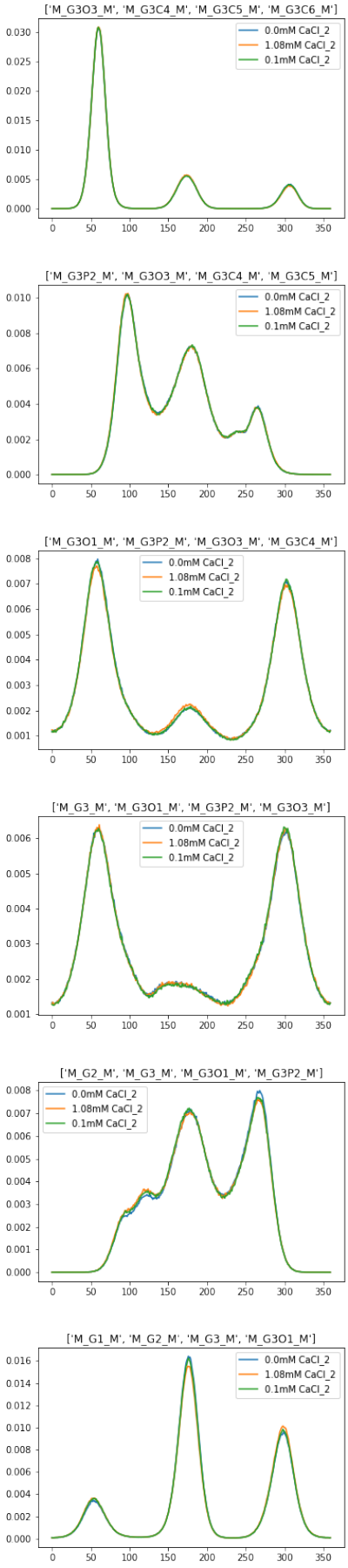

FIG. 6: Changes in POPG CHARMM36 dihedrals with increasing amount of $CaCl_2$.

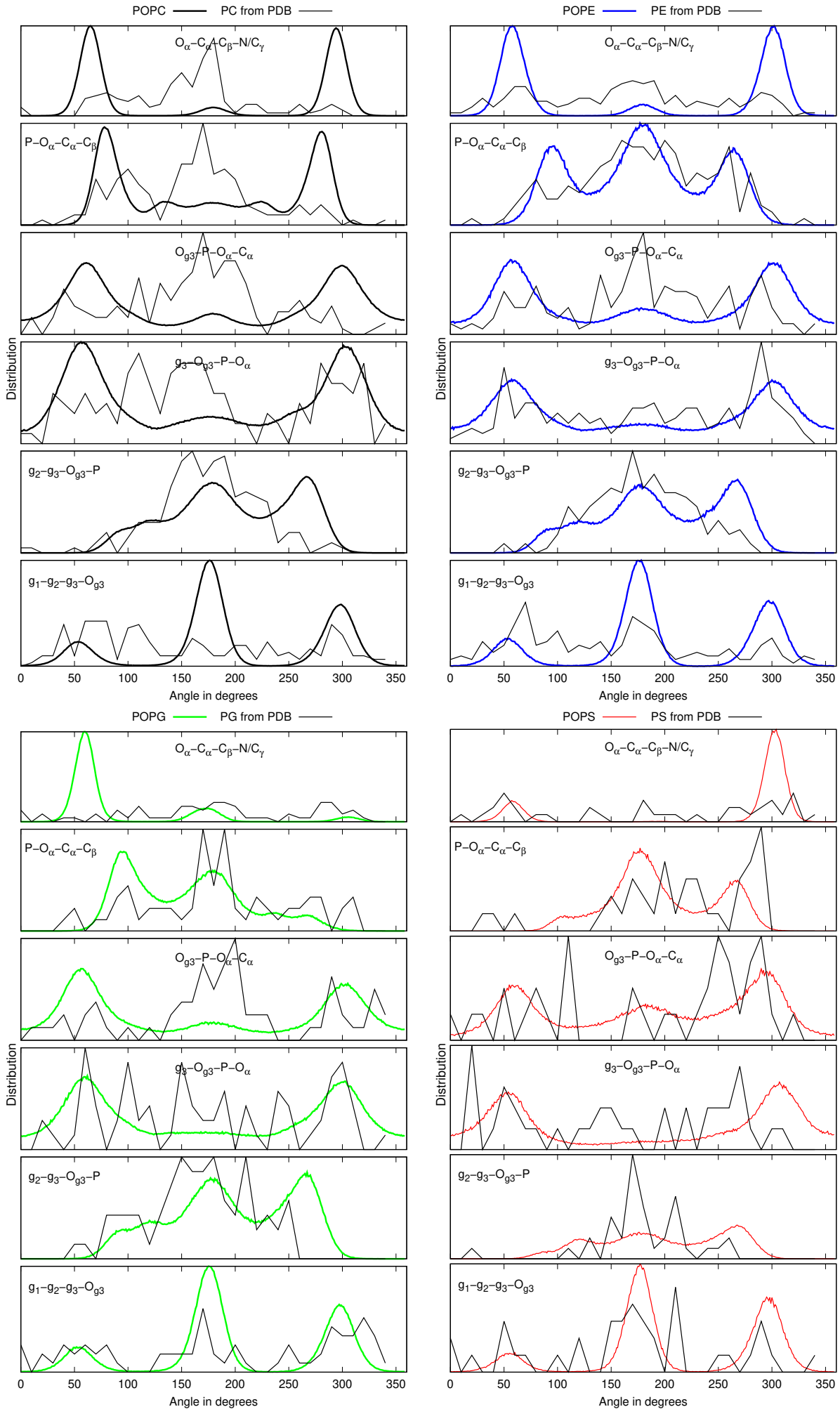

FIG. 7: Dihedral distributions from simulations and lipid structures in PDB.

CONCLUSIONS

AP is grateful to the Centro de Supercomputacin de Galicia (CESGA) for use of the Finis Terrae computer

* samuli.ollila@helsinki.fi

[1] C. Sohlenkamp and O. Geiger, FEMS Microbiology Reviews **40**, 133 (2015).

[2] J. E. Vance, Traffic **16**, 1 (2015).

[3] E. Calzada, O. Onguka, and S. M. Claypool (Academic Press, 2016), vol. 321 of *International Review of Cell and Molecular Biology*, pp. 29 – 88.

[4] D. Patel and S. N. Witt, Oxidative Medicine and Cellular Longevity **2017**, 4829180 (2017).

[5] S. Furse, Journal of Chemical Biology **10**, 1 (2017).

[6] P. Hariharan, E. Tikhonova, J. Medeiros-Silva, A. Jeucken, M. V. Bogdanov, W. Dowhan, J. F. Brouwers, M. Weingarth, and L. Guan, BMC Biology **16**, 85 (2018).

[7] P. L. Yeagle, Biochimica et Biophysica Acta (BBA) - Biomembranes **1838**, 1548 (2014), membrane Structure and Function: Relevance in the Cell's Physiology, Pathology and Therapy.

[8] L. V. Chernomordik and M. M. Kozlov, Nature Struct. Mol. Biol. **15**, 675 (2008).

[9] H. U. Gally, G. Pluschke, P. Overath, and J. Seelig, Biochemistry **20**, 1826 (1981).

[10] P. Scherer and J. Seelig, EMBO J. **6** (1987).

[11] J. Seelig, Cell Biology International Reports **14**, 353 (1990), ISSN 0309-1651, URL http://www.sciencedirect.com/science/article/pii/030916519091204H.

[12] R. Wohlgemuth, N. Waespe-Sarcevic, and J. Seelig, Biochemistry **19**, 3315 (1980).

[13] G. Büldt and R. Wohlgemuth, The Journal of Membrane Biology **58**, 81 (1981), ISSN 1432-1424, URL http://dx.doi.org/10.1007/BF01870972.

[14] J. Seelig, Q. Rev. Biophys. **10**, 353 (1977).

[15] J. H. Davis, Biochim. Biophys. Acta **737**, 117 (1983).

[16] D. J. Semchyschyn and P. M. Macdonald, Magn. Res. Chem. **42**, 89 (2004).

[17] A. Botan, F. Favela-Rosales, P. F. J. Fuchs, M. Javanainen, M. Kanduč, W. Kulig, A. Lamberg, C. Loison, A. Lyubartsev, M. S. Miettinen, et al., J. Phys. Chem. B **119**, 15075 (2015).

[18] H. S. Antila, P. Buslaev, F. Favela-Rosales, T. Mendes Ferreira, I. Gushchin, M. Javanainen, B. Kav, J. J. Madsen, J. Melcr, M. S. Miettinen, et al., The Journal of Physical Chemistry B p. acs.jpcb.9b06091 (2019), ISSN 1520-6106.

[19] A. H. de Vries, A. E. Mark, and S. J. Marrink, The Journal of Physical Chemistry B **108**, 2454 (2004).

[20] K. Murzyn, T. Rg, and M. Pasenkiewicz-Gierula, Biophysical Journal **88**, 1091 (2005), ISSN 0006-3495, URL http://www.sciencedirect.com/science/article/pii/S0006349505731799.

[21] U. R. Pedersen, C. Leidy, P. Westh, and G. H. Peters, Biochimica et Biophysica Acta (BBA) - Biomembranes **1758**, 573 (2006).

[22] W. Zhao, T. Rg, A. A. Gurtovenko, I. Vattulainen, and M. Karttunen, Biophysical Journal **92**, 1114 (2007), ISSN 0006-3495, URL http://www.sciencedirect.com/science/article/pii/S0006349507709232.

[23] A. A. Gurtovenko and I. Vattulainen, J. Phys. Chem. B **112**, 1953 (2008).

[24] W. Zhao, T. Rg, A. A. Gurtovenko, I. Vattulainen, and M. Karttunen, Biochimie **90**, 930 (2008), ISSN 0300-9084, URL http://www.sciencedirect.com/science/article/pii/S0300908408000692.

[25] J. Hnin, W. Shinoda, and M. L. Klein, The Journal of Physical Chemistry B **113**, 6958 (2009).

[26] A. Kukol, J. Chem. Theory Comput. **5**, 615 (2009).

[27] H.-H. G. Tsai, W.-X. Lai, H.-D. Lin, J.-B. Lee, W.-F. Juang, and W.-H. Tseng, Biochimica et Biophysica Acta (BBA) - Biomembranes **1818**, 2742 (2012), ISSN 0005-2736, URL http://www.sciencedirect.com/science/article/pii/S0005273612001873.

[28] C. J. Dickson, L. Rosso, R. M. Betz, R. C. Walker, and I. R. Gould, Soft Matter **8**, 9617 (2012).

[29] R. M. Venable, Y. Luo, K. Gawrisch, B. Roux, and R. W. Pastor, The Journal of Physical Chemistry B **117**, 10183 (2013).

[30] C. J. Dickson, B. D. Madej, A. A. Skjevik, R. M. Betz, K. Teigen, I. R. Gould, and R. C. Walker, J. Chem. Theory Comput. **10**, 865 (2014).

[31] N. A. Berglund, T. J. Piggot, D. Jefferies, R. B. Sessions, P. J. Bond, and S. Khalid, PLOS Computational Biology **11**, 1 (2015), URL https://doi.org/10.1371/journal.pcbi.1004180.

[32] G. Cevc, Biochim. Biophys. Acta - Rev. Biomemb. **1031**, 311 (1990).

[33] J.-F. Tocanne and J. Teissié, Biochim. Biophys. Acta - Reviews on Biomembranes **1031**, 111 (1990).

[34] M. Roux and M. Bloom, Biochemistry **29**, 7077 (1990).

[35] A. Catte, M. Girych, M. Javanainen, C. Loison, J. Melcr, M. S. Miettinen, L. Monticelli, J. Maatta, V. S. Oganesyan, O. H. S. Ollila, et al., Phys. Chem. Chem. Phys. **18**, 32560 (2016).

[36] J. Marra and J. Israelachvili, Biochemistry **24**, 4608 (1985).

[37] H. Hauser and G. Shipley, Biochimica et Biophysica Acta (BBA) - Biomembranes **813**, 343 (1985), ISSN 0005-2736, URL http://www.sciencedirect.com/science/article/pii/0005273685902512.

[38] G. W. Feigenson, Biochemistry **25**, 5819 (1986).

[39] M. Roux and M. Bloom, Biophys. J. **60**, 38 (1991).

[40] J. Melcr, H. Martinez-Seara, R. Nencini, J. Kolafa, P. Jungwirth, and O. H. S. Ollila, The Journal of Physical Chemistry B **122**, 4546 (2018).

[41] J. Melcr, T. Ferreira, P. Jungwirth, and O. H. S. Ollila, *Improved cation binding to lipid bilayer with negatively charged pops by effective inclusion of electronic polarization*, submitted, URL https://github.com/ohsOllila/ecc_lipids/blob/master/Manuscript/manuscript.pdf.

[42] S. V. Dvinskikh, H. Zimmermann, A. Maliniak, and D. Sandstrom, J. Magn. Reson. **168**, 194 (2004).

[43] J. D. Gross, D. E. Warschawski, and R. G. Griffin, J. Am. Chem. Soc. **119**, 796 (1997).

[44] T. M. Ferreira, F. Coreta-Gomes, O. H. S. Ollila, M. J. Moreno, W. L. C. Vaz, and D. Topgaard, Phys. Chem. Chem. Phys. **15**, 1976 (2013).

[45] T. M. Ferreira, R. Sood, R. Bärenwald, G. Carlström, D. Topgaard, K. Saalwächter, P. K. J. Kinnunen, and O. H. S. Ollila, Langmuir **32**, 6524 (2016).

[46] D. Marsh, *Handbook of Lipid Bilayers, Second Edition* (RSC press, 2013).

[47] J. Seelig and H. U. Gally, Biochemistry **15**, 5199 (1976).

[48] F. Borle and J. Seelig, Chemistry and Physics of Lipids **36**, 263 (1985).

[49] O. S. Ollila and G. Pabst, Biochimica et Biophysica Acta (BBA) - Biomembranes **1858**, 2512 (2016).

[50] N. Michaud-Agrawal, E. J. Denning, T. B. Woolf, and O. Beck-

stein, Journal of Computational Chemistry **32**, 2319 (2011), https://onlinelibrary.wiley.com/doi/pdf/10.1002/jcc.21787, URL https://onlinelibrary.wiley.com/doi/abs/10.1002/jcc.21787.

[51] Richard J. Gowers, Max Linke, Jonathan Barnoud, Tyler J. E. Reddy, Manuel N. Melo, Sean L. Seyler, Jan Domaski, David L. Dotson, Sbastien Buchoux, Ian M. Kenney, et al., in *Proceedings of the 15th Python in Science Conference*, edited by Sebastian Benthall and Scott Rostrup (2016), pp. 98 – 105.

[52] ohsOllila and et al., *Match github repository*, URL https://github.com/NMRLipids/MATCH.

[53] P. Fuchs and et al., *Buildh github repository*, URL https://github.com/patrickfuchs/buildH.

[54] T. J. Piggot, J. R. Allison, R. B. Sessions, and J. W. Essex, J. Chem. Theory Comput. **13**, 5683 (2017).

[55] M. Abraham, D. van der Spoel, E. Lindahl, B. Hess, and the GROMACS development team, *GROMACS user manual version 5.0.7* (2015), URL www.gromacs.org.

[56] J. L. Browning and J. Seelig, Biochemistry **19**, 1262 (1980).

[57] P. Mukhopadhyay, L. Monticelli, and D. P. Tieleman, Biophysical Journal **86**, 1601 (2004).

[58] M. Dahlberg, A. Marini, B. Mennucci, and A. Maliniak, The Journal of Physical Chemistry A **114**, 4375 (2010).

[59] P. M. Macdonald and J. Seelig, Biochemistry **26**, 1231 (1987).

[60] H. Akutsu and J. Seelig, Biochemistry **20**, 7366 (1981).

[61] J. Seelig, P. M. MacDonald, and P. G. Scherer, Biochemistry **26**, 7535 (1987).

[62] I. Leontyev and A. Stuchebrukhov, Phys. Chem. Chem. Phys. **13**, 2613 (2011).

[63] A. PEN, *CHARMM36 POPE Bilayer Simulation (Last 100 ns, 150 mM NaCl, 310 K)* (2019), URL https://doi.org/10.5281/zenodo.2577454.

[64] C. Par and M. Lafleur, Biophysical Journal **74**, 899 (1998), ISSN 0006-3495, URL http://www.sciencedirect.com/science/article/pii/S0006349598740135.

ToDo